Biochemistry and Biophysics Reports 38 (2024) 101676

Contents lists available at ScienceDirect

Biochemistry and Biophysics Reports

journal homepage: www.elsevier.com/locate/bbrep

The TGF-β/MMP9/RAGE axis induces sRAGE secretion by neutrophils and promotes oral carcinogenesis

Xiaolin Chen [a], Ningyuan Wang [a], Chenyang Jing [a], Jianghan Li [a], Xuanhao Liu [a], Yuquan Yang [a], Tianhuan Song [a], Hao Jia [a,b,*]

[a] Faculty of Basic Medicine, Shanghai Jiao Tong University School of Medicine, 280 South Chongqing Road, Shanghai, 200025, China
[b] Shanghai Key Laboratory for Tumor Microenvironment and Inflammation, Department of Biochemistry & Molecular Cellular Biology, Shanghai Jiao Tong University School of Medicine, Shanghai, 200025, China

ARTICLE INFO

Keywords:
Neutrophil
RAGE
MMP9
TGF-β
Oral leukoplakia
Oral squamous cell carcinoma

ABSTRACT

In the tumor microenvironment, transforming growth factor β (TGF-β) contributes to neutrophil development toward a pro-tumor phenotype; however, the molecular mechanism by which this occurs remains unclear. Therefore, we explored the role of TGF-β in N2 neutrophil polarization and the subsequent effect on oral leukoplakia/oral squamous cell carcinoma (OL/OSCC) cells. The TGF-β-stimulated N2 culture supernatant promoted the proliferation of OL/OSCC cells. Analysis of the N2 supernatant using a cytokine array revealed significantly upregulated expression of soluble forms of receptor for advanced glycation end products (RAGE). TGF-β was found to induce the expression of RAGE and matrix metalloproteinase 9 (MMP9) in neutrophils. Additionally, MMP9 treatment could cleave RAGE and promote its secretion by neutrophils, thereby promoting cancer cell proliferation. In an established mouse model of oral cancer using 4NQO, RAGE were found to be highly expressed. Importantly, neutralizing antibodies against RAGE significantly inhibited oral cancer progression in mice. Analysis of clinical data from the TCGA database revealed that RAGE and MMP9 are highly expressed in head and neck squamous cell carcinoma (HNSCC) and that RAGE expression is significantly positively correlated with neutrophil infiltration. In conclusion, our results indicate that TGF-β promotes N2 neutrophil polarization through upregulation of soluble RAGE (sRAGE) secretion, leading to OSCC cell proliferation. Our findings also suggest that the sRAGE formed during N2 polarization may be a potential therapeutic target in OL/OSCC.

1. Introduction

Transforming growth factor β (TGF-β) is an immunosuppressive cytokine positively correlated with chemoresistance; it triggers a signaling cascade which causes cancer cells to undergo epithelial-to-mesenchymal transition. TGF-β signaling mediates oncogene effects by promoting metastasis, angiogenesis, and immune escape [1]. Moreover, evidence suggests that TGF-β is overexpressed by tumor cells and plays a significant role in blocking immune responses and affecting tumor progression [2]. TGF-β blockers and TGF-β receptor inhibitors show anti-tumor effects mainly via the immune mechanism regulated by $CD8^+$ T cells. In addition to inhibiting T cell function, TGF-β also affects the function of myeloid cells. TGF-β contributes to the development of neutrophils toward a pro-tumor phenotype in the tumor microenvironment [3], although the underlying molecular mechanism by which this occurs remains unclear.

Neutrophils are the most abundant myeloid cells in human blood and are emerging as important tumor regulators. However, their functional importance is often overlooked because they are short-lived, terminally differentiated, and non-proliferative. Increasing studies have shown that tumor-associated neutrophils (TANs) play an important role in promoting tumors [4]. TANs are associated with lower survival rates in patients with melanoma [5], head and neck cancer [6], and hepatocellular carcinoma [7]. However, the mechanism by which TANs regulate

Abbreviations: TGF-β, transforming growth factor β; RAGE, receptor for advanced glycation end products; MMP9, matrix metalloproteinase 9; sRAGE, soluble RAGE; TANs, tumor-associated neutrophils; 4NQO, 4-nitroquinoline 1-oxide; TCGA, The Cancer Genome Atlas; OL, oral leukoplakia; OSCC, oral squamous cell carcinoma; HNSCC, head and neck squamous cell carcinoma.

* Corresponding author. Faculty of Basic Medicine, Shanghai Jiao Tong University School of Medicine, 280 South Chongqing Road, Shanghai, 200025, China.
E-mail address: fonney@sjtu.edu.cn (H. Jia).

https://doi.org/10.1016/j.bbrep.2024.101676
Received 18 January 2024; Received in revised form 27 February 2024; Accepted 27 February 2024

tumors remains unclear.

The receptor for advanced glycation end products (RAGE) is an important signaling receptor, and the downstream signaling pathway plays an important role in tumor occurrence and development [8–10]. RAGE can be expressed *in vivo* as a full-length membrane-bound form (fl-RAGE) or as various soluble forms lacking the transmembrane domain, collectively referred to as "soluble RAGE (sRAGE)". sRAGE can be divided into two categories according to its source: cRAGE, cleaved from fl-RAGE, and endogenously secreted esRAGE [11]. However, the role of sRAGE in tumors remains unclear.

In this study, we established a mouse model of oral leukoplakia (OL)/oral squamous cell carcinoma (OSCC) and investigated the mechanisms through which TGF-β promotes neutrophil polarization to N2 in the tumor cells. Based on the results of a cytokine array analysis, we further examined the role of TGF-β-induced RAGE and matrix metalloproteinase 9 (MMP9) in tumor cell proliferation. We also investigated their role in a mouse model of oral cancer and determined the therapeutic efficacy of neutralizing antibodies against RAGE in this mouse model. Our study provides insights into the mechanisms regulating oral carcinogenesis and reveals relevant targets for tumor treatment.

2. Materials and methods

2.1. Cell culture and drugs

DOK, Cal27, SCC25 and HN4 cells were cultured in DMEM supplemented with 10% fetal bovine serum at 37 °C in a humidified atmosphere with 5% CO_2. All cells were obtained from the ATCC. Information on the drugs used is presented in Supplementary Table 1.

2.2. Cell viability

Cell viability was assessed using a CCK-8 assay kit as previously described [12]. For the assay, 1×10^4 cells per well were seeded in 96-well plates, and the absorbance was measured at 480 nm against a background control using a microplate reader.

2.3. Neutrophil isolation

Neutrophils were isolated by density gradient centrifugation, according to the manufacturer's guidelines (Solarbio, P8550). Briefly, the femurs and tibias of mice were extracted aseptically, and the bone marrow cavity was rinsed to obtain the bone marrow. The obtained single-cell suspension was then carefully overlaid onto the surface of the density gradient separation solution and centrifuged for 30 min at 1000×*g* in a horizontal rotor at room temperature. After centrifugation, two circular milky-white cell layers were observed in the tubes; collect the lower layer to obtain neutrophils. To collect the conditioned medium (CM), neutrophils were cultured at a concentration of 4×10^6 cells/mL with TGF-β at 40 ng/mL for 4 h, and the CM was collected after centrifugation (4 °C, 13000×*g*, 20 min).

2.4. Enzyme-linked immunosorbent assay (ELISA)

Neutrophils were cultured at a concentration of 4×10^6 cells/mL, with or without TGF-β (40 ng/mL) for 4 h, and supernatants were collected. The concentration of sRAGE in the culture supernatant was detected using ELISA kits according to the manufacturer's instructions (Jiangsu Meimian industrial Co., Ltd, China).

2.5. Cytokine array analysis

Cytokine array analysis was performed using a Label-Based (L-Series) Mouse L308 Array Kit according to the manufacturer's standard operating procedures (H-Wayen Biotechnologies, Shanghai, China). Briefly, the samples were first purified using spin columns and then biotin-labeled. Glass slides were removed from the refrigerator and equilibrated to room temperature. After the glass slides were completely dried, blocking and incubations were performed. Fluorescence detection was performed after the incubation.

2.6. Immunofluorescence staining

Paraffin-embedded and formalin-fixed samples were cut into 5-μm sections, which were then processed for immunofluorescent staining or immunohistochemical staining. The sections were incubated with antibodies against mouse RAGE (ab-3611, abcam, USA), followed by incubation with Alexa Fluor 488 goat anti-rabbit IgG (Invitrogen). Subsequently, images were acquired using a confocal microscope (Zeiss LSM 710, Carl Zeiss, Dublin, CA, USA).

2.7. Modified mouse tongue leukoplakia/SCC model treated with RAGE monoclonal antibody therapy

Eight-week-old male C57BL/6J mice were purchased from Shanghai Lingchang Biotechnology Science and Technology (China) and used to establish an OL/OSCC model. Briefly, a 100 μg/mL solution of the carcinogen 4NQO (Sigma, St. Louis, MO, USA) was prepared in double-distilled water (ddH_2O) with overnight stirring at room temperature. Thereafter, the mice were given the 4NQO solution instead of drinking water. The RAGE monoclonal antibody (mAb) treatment method used for each cage is shown in Fig. 3E.

2.8. RNA-seq and validation by qRT-PCR

Total RNA was extracted from cultured cells and tissue samples using TRIzol reagent, according to the manufacturer's protocol (TaKaRa, Dalian, Japan). For microarray analysis, the Affymetrix (Santa Clara, CA, USA) Gene ChipR Human Transcriptome Array 2.0 was employed according to the manufacturer's protocol. RNA-seq of the samples was performed on an Illumina HiSeq X Ten sequencing system and detected using Novogene (Liebing Bioinformatics Technology, China).The primers sequences in Supplementary Table 2.

2.9. Statistical analysis

Results are expressed as mean values ± standard errors of mean. Statistical analyses were performed using GraphPad Prism software version 6.1 (La Jolla, CA, USA). The statistical significance of differences between groups was determined using Student's *t*-test. All data were analyzed using two-tailed tests unless otherwise specified, and statistical significance was set at $P < 0.05$.

3. Results

3.1. Tumor-associated neutrophils promote RAGE-dependent proliferation of OL and OSCC cells

For tumor-associated neutrophil (TAN) induction, primary neutrophils were treated with TGF-β (40 ng/mL) for 24 h. qRT-PCR analysis indicated that the markers *CCL2*, *Arg2*, and *YM1* were elevated, confirming the transformation of monocytes into N2-type neutrophils (Fig. 1A–C). Cell proliferation assay showed that co-culture with N2 superntant facilitated the growth of DOK and HN4 cells compared to co-culture with N0 superntant (Fig. 1D–F). To understand the mechanism by which the N2 supernatant promotes OL and OSCC cell proliferation and metastasis, we performed a cytokine array analysis. The results showed that the expression of several cytokines was upregulated (Fig. 1G), with RAGE showing significantly upregulated expression (Fig. 1H). To confirm the cytokine array findings, we performed ELISA, which showed that the levels of RAGE were increased in the N2 supernatant compared with those in the ctrl group (Fig. 1I). To determine

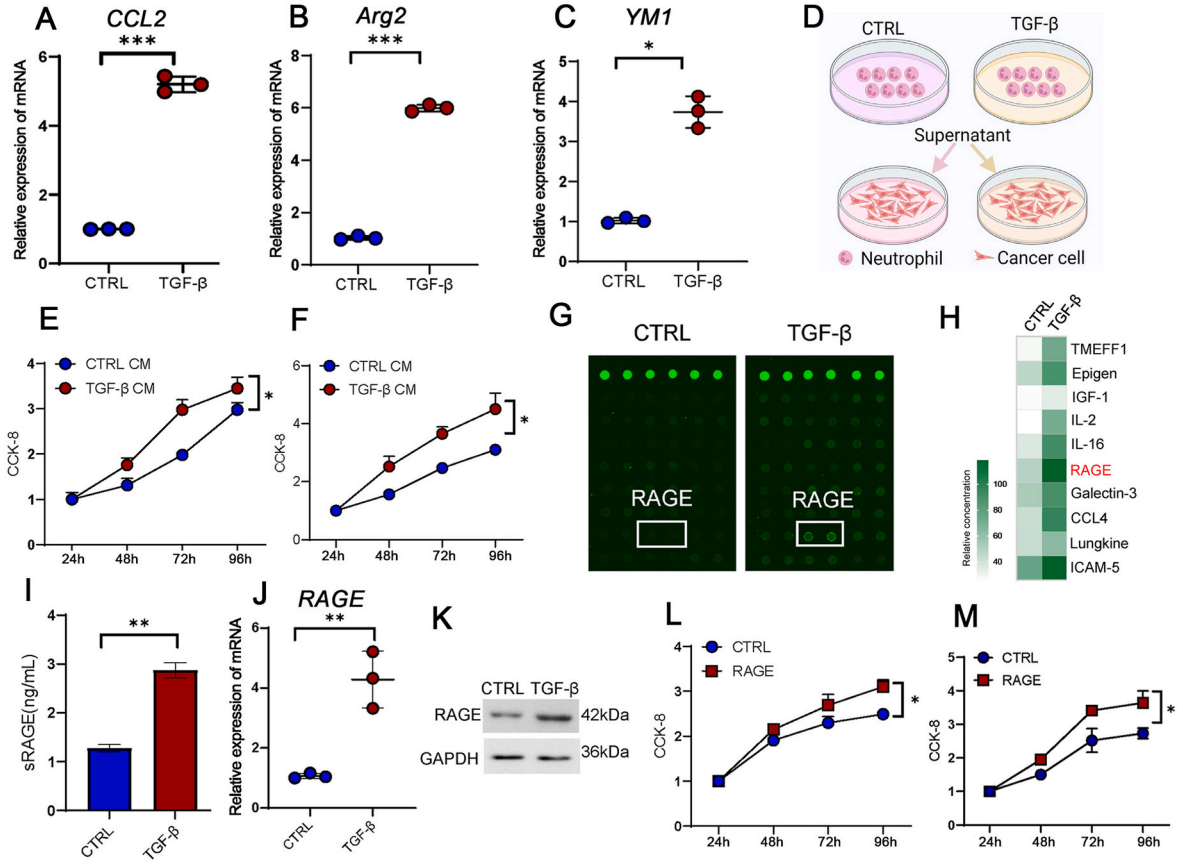

Fig. 1. TGF-β-induced N2 neutrophil polarization, and N2 supernatant promotes tumor cell proliferation dependent on RAGE.
A-C. qRT-PCR analysis of *CCL2*, *Arg2*, and *YM1* expression in TGF-β-stimulated mouse primary neutrophils. **D**. Schematic diagram of treatment of OL/OSCC cells with N2 neutrophil culture supernatant. **E-F**. CCK-8 assay showing cell proliferation of DOK (E) and HN4 (F) cells post treatment with the N2 culture supernatant. **G**. Cytokine array analysis showing significant changes in the expression of multiple proteins. **H.** RAGE exhibits a robust increase in the TGF-β treatment group compared to that in the CTRL group. **I**. RAGE expression in N2 culture supernatant detected using ELISA. Induction of RAGE in neutrophils by TGF-β confirmed using **J** qRT-PCR and **K** western blotting. CCK-8 assay showing cell proliferation of **L** Cal27 and **M** SCC25 cells post treatment with RAGE. Data in A-C, E, F, I, J, L, and M are shown as mean ± SD from three independent experiments; $*P < 0.05$. $**P < 0.01$. $***P < 0.001$.

whether TGF-β is involved in the regulation of RAGE expression, we examined the expression of RAGE in TGF-β-stimulated neutrophil cells. Both qRT-PCR and western blotting confirmed that TGF-β treatment induced RAGE expression in N2 cells (Fig. 1J and K). Furthermore, compared to the ctrl group, the RAGE group had a significant proliferative effect on OSCC cells (Fig. 1L and M).

3.2. *TGF-β promotes MMP9 expression to cleave sRAGE*

RAGE is a 55 kDa type I membrane glycoprotein receptor of the immunoglobulin superfamily. In the current study, the soluble form of RAGE, sRAGE, was detected in the cell culture medium. As previous studies have shown that MMP9 can cleave RAGE to form sRAGE, we further examined the expression of MMP9 after TGF-β treatment of neutrophils. The results indicated that MMP9 was indeed upregulated by TGF-β (Fig. 2A and B). Furthermore, post addition of MMP9 protein to TGF-β-treated neutrophils, sRAGE was detected in the cell culture supernatant (Fig. 2C). To identify the downstream targets of TGF-β that regulate N2, RNA-seq was performed to identify target genes involved in the regulation of MMP9 and RAGE expression. We then used ChIP-seq data of MMP9 and RAGE from the database and conducted an overlapping analysis with the RNA-seq database to screen candidate transcription factors (Fig. 2D and H). Further, using qRT-PCR, TGF-β was found to upregulate RAGE expression via *Bhlhe40* (Fig. 2E–G) and MMP9 expression via *Mxi1* (Figs. 2I-3K). Taken together, these results indicated that TGF-β-induced MMP9 cleaves RAGE to form sRAGE in N2 cells.

3.3. *RAGE mAb treatment in oral tongue tumor mouse model*

To clarify RAGE involved in OSCC progression, mice were treated with 4NQO (Fig. 3A). Typical tongue tumor was observed in the 4NQO group by macroscopic observation and H&E staining (Fig. 3B and C). Then immunofluorescence (IF) was performed, RAGE staining were found to be stronger in OL(4NQO) than in normal mucosa (PBS) (Fig. 3D). To verify whether MMP9-cleaved RAGE from neutrophils promotes the proliferation of oral cancer cells, we used RAGE mAb to treat 4NQO-induced oral tongue cancer in mice (Fig. 3E). The results showed that after RAGE mAb treatment, the number of mouse-tongue tumors smaller than 1 mm were significantly reduced (Fig. 3F–K), whereas the number of tumors larger than 1 mm at the beginning of the treatment showed no significant change.

3.4. *RAGE and MMP9 are highly expressed in tumors*

We analyzed the *RAGE* and *MMP9* mRNA expression recorded in The Cancer Genome Atlas (TCGA) datasets to further explore the clinical relevance of these genes in patients with malignant tumors, and found that *RAGE* (Fig. 4A) and *MMP9* (Fig. 4E) transcripts were overexpressed in most carcinoma tissues compared to that in non-cancerous tissues. In addition, the mRNA levels of *RAGE* (Fig. 4B) and *MMP9* (Fig. 4F) in patients with head and neck squamous cell carcinoma (HNSCC) were

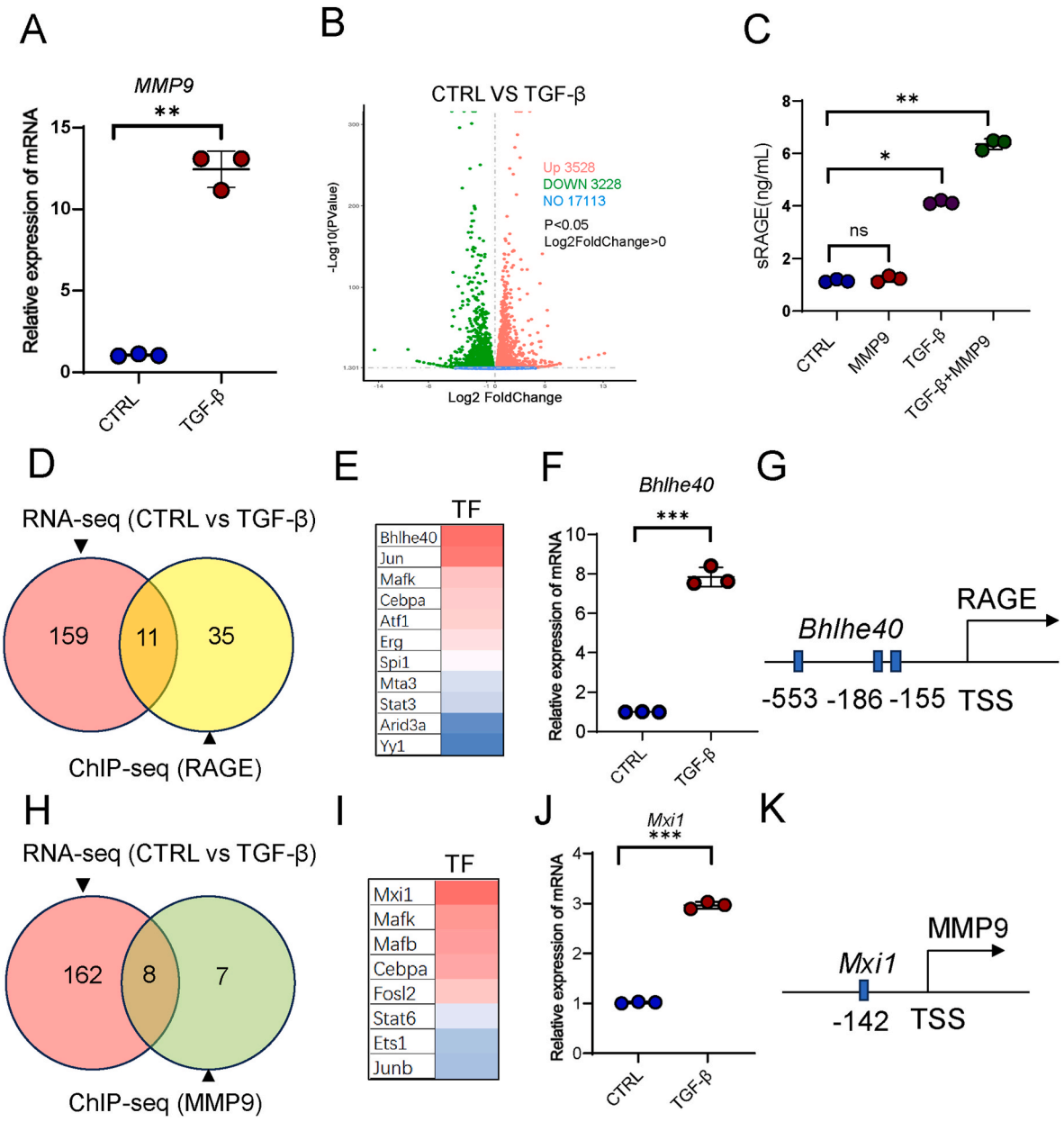

Fig. 2. TGF-β can induce the expression of MMP9 and RAGE, and highly expressed MMP9 can cleave RAGE to form sRAGE. **A**. qRT-PCR analysis of *MMP9* expression in TGF-β-stimulated mouse primary neutrophils. **B**. The Volcano Plot analysis of the differentially expressed genes in TGF-β and CTRL neutrophil identified by the RNA-seq approach. Red dots represent genes induced by TGF-β, green dots represent genes repressed by TGF-β, and blue dots represent genes without significant difference. **C.** ELISA analysis showing sRAGE expression in N2 supernatant treated with MMP9. **D-E**. ChIP-seq of RAGE in the database and overlapping analysis with the RNA-seq database to screen out 11 candidate transcription factors. **F-G**. qRT-PCR analysis of *Bhlhe40* expression in TGF-β-stimulated mouse primary neutrophils. **H-I**. ChIP-seq of MMP9 in the database and overlapping analysis with the RNA-seq database to screen out 8 candidate transcription factors. **J-K**. qRT-PCR analysis of *Mxi1* expression in TGF-β-stimulated mouse primary neutrophils. Data in A, B, E, and F are shown as mean ± SD from three independent experiments; $^{*}P < 0.05$. $^{**}P < 0.01$. $^{***}P < 0.001$. ns, not significant.

significantly higher in tumor tissues than in matched adjacent normal tissues. In HNSCC samples, *RAGE* (Fig. 4C) and *MMP9* (Fig. 4G) expression level had a clear positive correlation with neutrophil infiltration level. Information on the baseline characteristics of the patients included in the data analysis is shown in Supplementary Table 3. Kaplan–Meier survival analysis showed that patients with high RAGE (Fig. 4D) and MMP9 (Fig. 4H) levels had shorter survival times than those with low RAGE levels. We further analyzed the relationship between RAGE and MMP9 expression in tumor from HNSCC samples. Pearson's correlation analysis revealed a positive correlation between RAGE and MMP9 levels in HNSCC samples (Fig. 4I). Moreover, these results suggest that the upregulation of RAGE and MMP9 is significantly associated with advanced progression of HNSCC.

4. Discussion

TANs are considered to have a key role in tumor formation and angiogenesis [2,13]. Numerous functional studies have shown that tumors can stimulate neutrophils to promote angiogenesis, migration, and the invasion of tumor cells. Tumor cells can secrete TGF-β, which further promotes the polarization of neutrophils in the tumor microenvironment into N2 populations with a pro-tumor phenotype [2], which can promote the proliferation and metastasis of tumor cells through the secretion of some cytokines associated with feedback, but the

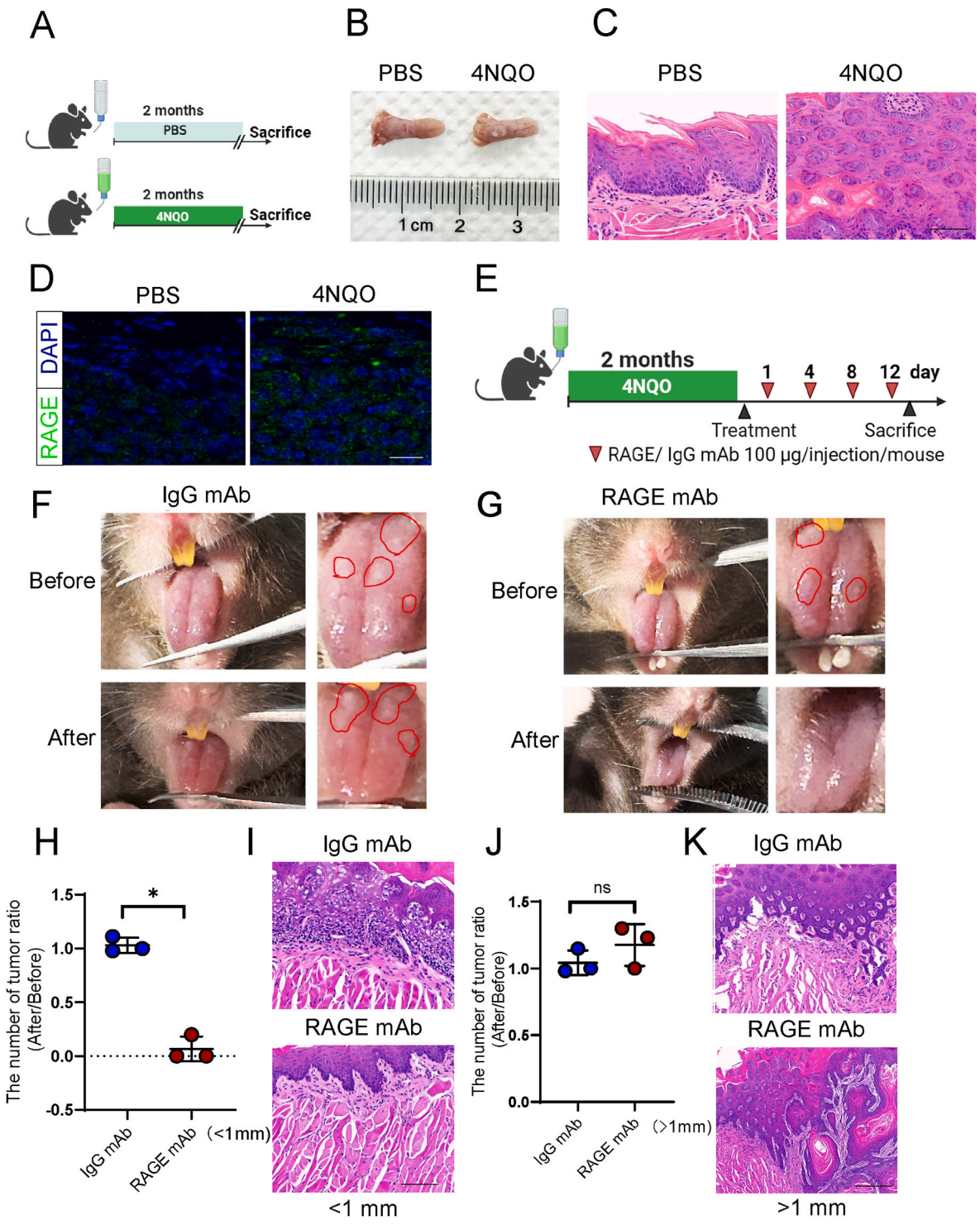

Fig. 3. RAGE mAb treatment in oral tongue tumor mouse model. **A**. Schematic timeline of the 4NQO treatment in tongue leukoplakia mouse model. **B**. Macroscopic view of the tongue of mice in the PBS and 4NQO groups. **C.** Typical tongue leukoplakia and SCC in the 4NQO group. Histopathological diagnosis confirming leukoplakia on the dorsal tongue and local early invasive tongue SCC in the 4NQO group (200 ×). **D**. Immunofluorescence showing RAGE staining in the 4NQO and control (PBS) groups (200 ×). **E**. Schematic timeline of the RAGE mAb treatment in early tongue leukoplakia mouse model. **F-G**. RAGE mAb is effective in leukoplakia treatment, especially for leukoplakia induced by 4NQO. Macroscopic view before and after RAGE (F)/IgG (G) mAb treatment. **H-K**. Ratio of tongue lesion score before and after RAGE mAb treatment (200 ×). Data in H and J are shown as mean ± SD from three independent experiments; $^{*}P < 0.05$. ns, not significant.

mechanism is still unclear. To answer this question, TGF-β-treated neutrophil supernatants were cultured with OSCC cells, mimicking a paracrine form of the tumor microenvironment. As a result, TGF-β-treated neutrophil supernatants could significantly increase OL (DOK)/OSCC (HN4) cell proliferation. TANs exhibit an exceptional cytokine profile, and they secrete cytokines such as CXCL10, IL23a, and ARG1 [14]. However, the types of cytokines are not sufficiently understood, and thus, we used the cytokine array of L308 samples for screening, to identify the most abundant cytokines. Furthermore, the expression of RAGE was detected in our study. RAGE is expressed in

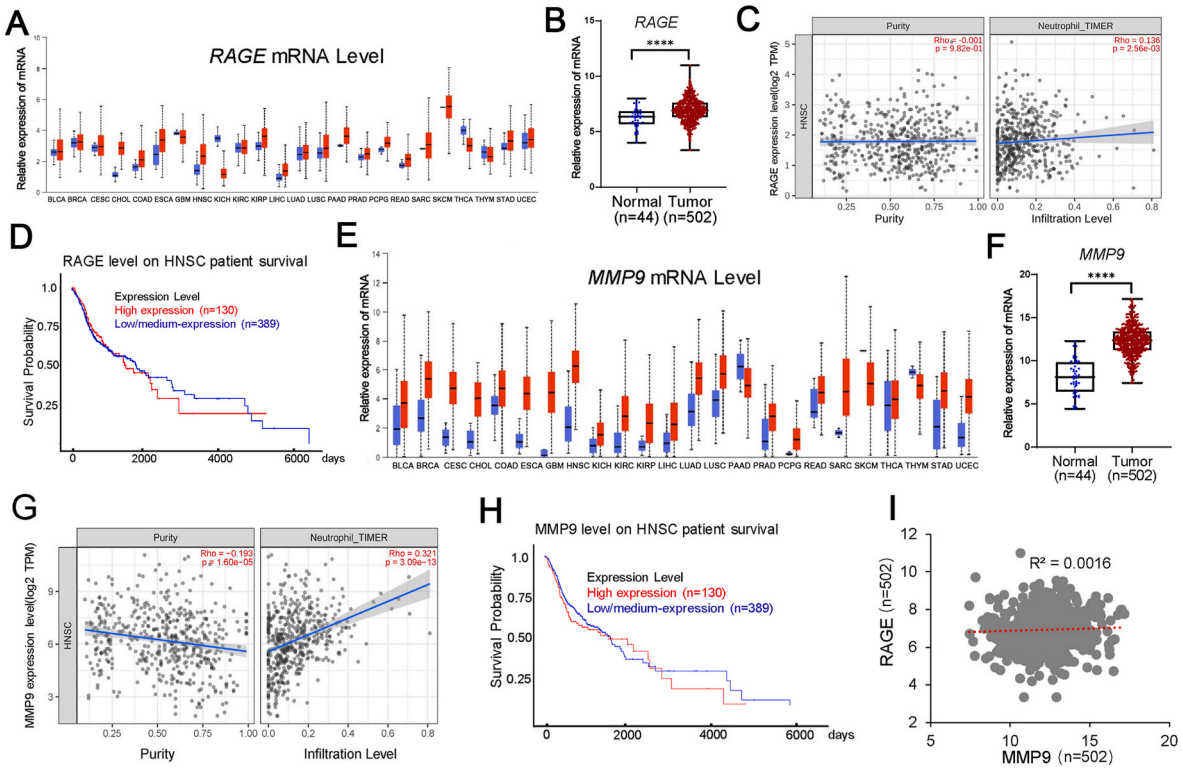

Fig. 4. RAGE and MMP9 are highly expressed in HNSC. **A**. The Cancer Genome Atlas (TCGA) data showing levels of *RAGE* transcripts in carcinoma tissues and noncancerous tissues. **B**. TCGA data showing expression of *RAGE* in HNSCC tissues (n = 502) and normal tissues (n = 44).**C.** Correlations between *RAGE* expression and infiltrating neutrophil levels. **D**. Kaplan–Meier survival analysis of patients with high *RAGE* levels compared to those with low RAGE levels. **E**. The Cancer Genome Atlas (TCGA) data showing levels of *MMP9* transcripts in carcinoma tissues and noncancerous tissues. **F.** TCGA data showing expression of *MMP9* in HNSCC tissues (n = 502) and normal tissues (n = 44). **G**. Correlations between *MMP9* expression and and infiltrating neutrophil levels. **H**. Kaplan–Meier survival analysis of patients with high *MMP9* levels compared to those with low *MMP9* levels. **I**. Correlation between the levels of *RAGE* and *MMP9* in HNSCC tissues. ****$P < 0.0001$.

many tumor cell types, and its activation is closely related to tumor growth [9], cell migration [15], cell death [8], angiogenesis [9], and resistance to occlusion. Recent studies have shown that HMGB1, which is abundantly expressed in the tumor microenvironment, can promote the polarization of macrophages toward M2 through the RAGE signaling pathway, enhancing tumor cell invasion, new vascular network formation, and MMP9 production [16]. The role of RAGE in N2 polarization has not been studied yet. In addition, studies have found that RAGE affects the tumor microenvironment and promotes the occurrence of tumor-related cytokines. The source of RAGE in the tumor microenvironment is unclear. Our study found that RAGE in the tumor microenvironment originates from neutrophils. Furthermore, we used RNA-seq and bioinformatics analyses to determine that the transcription factor *Bhlhe40* can upregulate the expression of RAGE and that *Mxi1* can upregulate the expression of MMP9, which was also verified in neutrophils. The optimal clinical treatments for OL and OSCC remain unsatisfactory, and there are no effective treatments for preventing the development of oral cancer. Our previous study showed that PD-1 mAb can block oral carcinogenesis [12], althought the response rate is only 50%. Based on this, we used RAGE mAb to treat 4NQO-induced oral tongue cancer in mice, the results showed that the mouse-tongue tumors smaller than 1 mm were significantly reduced. However, there is no significant effect on large tumors.

As shown in the graphical abstract, in our study, we found that treating neutrophils with TGF-β upregulated the expression of MMP9 and RAGE. The upregulated MMP9 cleaved RAGE to form sRAGE, which contributed to the proliferation and metastasis of OL/OSCC cells. More importantly, RAGE mAb was effective for OSCC treatment in mice. These results suggest that the RAGE/MMP9 axis in N2 neutrophil polarization could be a promising therapeutic target for OL and OSCC. In the future, a combination therapy of RAGE mAb and PD-1 mAb may could yield good results.

Funding

This work was supported by the Shanghai Rising-Star Program (19QA1405000), and the Innovative research team of high-level local universities in Shanghai (SHSMU-ZDCX20211801).

Ethics statement

All animal experiments were carried out following the protocols approved by Experimental Animal Center of shanghai Jiao Tong University (SCXK [Shanghai 2007–0005]). Mice described in our experiment were obtained from Experimental animal center.

CRediT authorship contribution statement

Xiaolin Chen: Writing – original draft, Resources, Project administration, Methodology, Data curation. **Ningyuan Wang:** Supervision, Software, Project administration, Methodology. **Chenyang Jing:** Validation, Project administration, Methodology. **Jianghan Li:** Methodology. **Xuanhao Liu:** Methodology, Data curation. **Yuquan Yang:** Methodology, Investigation. **Tianhuan Song:** Project administration, Methodology. **Hao Jia:** Writing – review & editing, Investigation, Data curation, Conceptualization.

Declaration of competing interest

The authors have no conflict of interest.

Acknowledgments

The authors would like to thank Editage (www.editage.cn) for English language editing. The authors thank Professor Linjun Shi from the Department of Oral Pathology of Shanghai Ninth People's Hospital for histopathological diagnosis.

Appendix A. Supplementary data

Supplementary data to this article can be found online at https://doi.org/10.1016/j.bbrep.2024.101676.

References

[1] B. Bierie, H.L. Moses, Tumour microenvironment: TGFbeta: the molecular Jekyll and Hyde of cancer, Nat. Rev. Cancer 6 (2006) 506–520, https://doi.org/10.1038/nrc1926.

[2] Z.G. Fridlender, J. Sun, S. Kim, V. Kapoor, G. Cheng, L. Ling, G.S. Worthen, S. M. Albelda, Polarization of tumor-associated neutrophil phenotype by TGF-beta: "N1" versus "N2" TAN, Cancer Cell 16 (2009) 183–194, https://doi.org/10.1016/j.ccr.2009.06.017.

[3] G.L. Burn, A. Foti, G. Marsman, D.F. Patel, A. Zychlinsky, The neutrophil, Immunity 54 (2021) 1377–1391, https://doi.org/10.1016/j.immuni.2021.06.006.

[4] M.E. Shaul, Z.G. Fridlender, Tumour-associated neutrophils in patients with cancer, Nat. Rev. Clin. Oncol. 16 (2019) 601–620, https://doi.org/10.1038/s41571-019-0222-4.

[5] T.O. Jensen, H. Schmidt, H.J. Moller, F. Donskov, M. Hoyer, P. Sjoegren, I. J. Christensen, T. Steiniche, Intratumoral neutrophils and plasmacytoid dendritic cells indicate poor prognosis and are associated with pSTAT3 expression in AJCC stage I/II melanoma, Cancer 118 (2012) 2476–2485, https://doi.org/10.1002/cncr.26511.

[6] S. Trellakis, K. Bruderek, C.A. Dumitru, H. Gholaman, X. Gu, A. Bankfalvi, A. Scherag, J. Hutte, N. Dominas, G.F. Lehnerdt, T.K. Hoffmann, S. Lang, S. Brandau, Polymorphonuclear granulocytes in human head and neck cancer: enhanced inflammatory activity, modulation by cancer cells and expansion in advanced disease, Int. J. Cancer 129 (2011) 2183–2193, https://doi.org/10.1002/ijc.25892.

[7] Y.W. Li, S.J. Qiu, J. Fan, J. Zhou, Q. Gao, Y.S. Xiao, Y.F. Xu, Intratumoral neutrophils: a poor prognostic factor for hepatocellular carcinoma following resection, J. Hepatol. 54 (2011) 497–505, https://doi.org/10.1016/j.jhep.2010.07.044.

[8] G.P. Sims, D.C. Rowe, S.T. Rietdijk, R. Herbst, A.J. Coyle, HMGB1 and RAGE in inflammation and cancer, Annu. Rev. Immunol. 28 (2010) 367–388, https://doi.org/10.1146/annurev.immunol.021908.132603.

[9] A. Taguchi, D.C. Blood, G. del Toro, A. Canet, D.C. Lee, W. Qu, N. Tanji, Y. Lu, E. Lalla, C. Fu, M.A. Hofmann, T. Kislinger, M. Ingram, A. Lu, H. Tanaka, O. Hori, S. Ogawa, D.M. Stern, A.M. Schmidt, Blockade of RAGE-amphoterin signalling suppresses tumour growth and metastases, Nature 405 (2000) 354–360, https://doi.org/10.1038/35012626.

[10] H.S. Hofmann, G. Hansen, S. Burdach, B. Bartling, R.E. Silber, A. Simm, Discrimination of human lung neoplasm from normal lung by two target genes, Am. J. Respir. Crit. Care Med. 170 (2004) 516–519, https://doi.org/10.1164/rccm.200401-127OC.

[11] L.J. Sparvero, D. Asafu-Adjei, R. Kang, D. Tang, N. Amin, J. Im, R. Rutledge, B. Lin, A.A. Amoscato, H.J. Zeh, M.T. Lotze, RAGE (Receptor for Advanced Glycation Endproducts), RAGE ligands, and their role in cancer and inflammation, J. Transl. Med. 7 (2009) 17, https://doi.org/10.1186/1479-5876-7-17.

[12] L. Shi, Y. Yang, M. Li, C. Li, Z. Zhou, G. Tang, L. Wu, Y. Yao, X. Shen, Z. Hou, H. Jia, LncRNA IFITM4P promotes immune escape by up-regulating PD-L1 via dual mechanism in oral carcinogenesis, Mol. Ther. 30 (2022) 1564–1577, https://doi.org/10.1016/j.ymthe.2022.01.003.

[13] X. Zhan, R. Wu, X.H. Kong, Y. You, K. He, X.Y. Sun, Y. Huang, W.X. Chen, L. Duan, Elevated neutrophil extracellular traps by HBV-mediated S100A9-TLR4/RAGE-ROS cascade facilitate the growth and metastasis of hepatocellular carcinoma, Cancer Commun. 43 (2023) 225–245, https://doi.org/10.1002/cac2.12388.

[14] N. Roussot, F. Ghiringhelli, C. Rebe, Tumor immunogenic cell death as a mediator of intratumor CD8 T-cell recruitment, Cells 11 (2022), https://doi.org/10.3390/cells11223672.

[15] M.C. Chen, K.C. Chen, G.C. Chang, H. Lin, C.C. Wu, W.H. Kao, C.J. Teng, S.L. Hsu, T.Y. Yang, RAGE acts as an oncogenic role and promotes the metastasis of human lung cancer, Cell Death Dis. 11 (2020) 265, https://doi.org/10.1038/s41419-020-2432-1.

[16] C. Hou, M. Lu, Z. Lei, S. Dai, W. Chen, S. Du, Q. Jin, Z. Zhou, H. Li, HMGB1 positive feedback loop between cancer cells and tumor-associated macrophages promotes osteosarcoma migration and invasion, Lab. Invest. 103 (2023), https://doi.org/10.1016/j.labinv.2022.100054.